Finkelstein, M., Yoo, N. Y., & Cha, J. H. (2025). Discussing cascading failures: The bursting point processes approach. Applied Stochastic Models in Business and Industry, 41(6), Article e70060. https://doi.org/10.1002/asmb.70060. For the purpose of open access, a CC BY 4.0 licence has been applied.

Discussing Cascading Failures: the Bursting Point Processes Approach

Maxim Finkelstein[a,b], Na Young Yoo[c], Ji Hwan Cha[1,d]

[a] Department of Mathematical Statistics, University of the Free State, Bloemfontein, South Africa
E-mail: FinkelM@ufs.ac.za

[b] Department of Management science, University of Strathclyde, Glasgow, UK

[c]Department of Statistics, Ewha Womans University, Seoul, 120-750, Rep. of Korea.
E-mail: fullmoon16@ewha.ac.kr

[d]Department of Statistics, Ewha Womans University, Seoul, 120-750, Rep. of Korea.
E-mail: jhcha@ewha.ac.kr

Abstract. We discuss the new approach to modelling cascading failures from a probabilistic viewpoint based on exploding self-exciting point processes. It explains a *possible mechanism* of the cascade development. From the practical point of view, this approach might be oversimplified for modelling the flow of events (failures) in, for example, real-life power grids (as, e.g., not considering the specific network topology). However, even in this general form, it can be useful for overall modelling of the converging process of cascading failures and understanding the probabilistic nature of this interesting phenomenon. Three baseline processes are considered: the geometric process, the geometric-type process with a decreasing threshold after each event and the extended generalized Polya process.

Keywords: Cascading failures; self-exciting processes; bursting processes; geometric process; extended generalized Polya process

1. Introduction

Interactions and inter-dependences between various components and units of modern complex system along with sophisticated controlling functions can significantly increase the likelihood of subsequent failures of other components after the initial failure, human or logistic error or external impacts. When, for example, one component fails, the failure might 'propagate' and cause failures of other components. This phenomenon is known as a cascading failure. Cascading failures in practice can occur in electric power transmission systems, transportation systems, communication systems and other complex network systems. Electric power-systems are one of the most important critical infrastructures in modern society. In recent years, they have been exposed to extreme stress due to the increasing demand, the introduction of distributed renewable energy sources, and the development of extensive interconnections (Pahwa et al[1]). Damage of a node could trigger an overload on other components of the grid that further propagates to the entire system that could lead to a catastrophic collapse of the

[1] Corresponding Author

system. The initial failure/event that triggers the cascade could be due to human attacks or natural disasters such as hurricanes or lightnings, etc., as the tsunami in Japan in 2011, and the forest fire in California in August 2018 (Valdez et al[2]).

There are not so many existing publications in the relevant literature within reliability context describing probabilistic mechanism that can result in cascading failures. For instance, Swift[3] and Lee and Cha[4] provide explicit reliability modelling for redundant systems with load sharing (parallel system with two components and k out of n systems, respectively) when a failure of a component increases the load (and thus the probability of failure) of remaining components. This impact lasts for a limited time and then the increased load is back to its initial level (a sort of repair action). However, in the framework of a conventional reliability theory, those are just cases of dependent (via the specific load sharing mechanism) components of a system.

Thus, in essence, the term "cascading" can be misleading for the above setting, as most often, e.g., in power grids, it means the sequence of failures/defects usually resulting in the relatively abrupt collapse of the grid (Pahwa et al[1]). For example, during the European blackout in 2006, a total of 33 high-voltage transmission lines tripped within a time period of 1 min and 20 seconds, with 30 of those lines failing within the first 19 seconds (Schäfer et al[5]). See also Motter and Lai[6], Liu et al[7], Song et al[8], Valdez et al[2] among others for relevant discussions.

The reliability-wise approaches considered in Swift[3] and Lee and Cha[4], obviously, were not developed for modelling this type of failures/defects sequences converging to the collapsing state. On the other hand, e.g., Song et al[9] and Zhao et al[10] provide analysis of cascading failures based on combination of the simplified reliability modelling with simulations but also not reflecting this sequential mechanism. Schäfer et al[5] describe the cascading failure in the following way: "Complex networks are also prone to cascading failures. In these events, the failure of a component triggers the successive failures of other parts of the network. In this way, an initial local 'shock' produces a sequence of multiple failures in a domino mechanism which may finally affect a substantial part of the network".

As far as we know, the existing models describing the development of cascading failures do not suggest a general probabilistic mechanisms of the rapid development of these catastrophic events. They discuss specific models with given failure thresholds or criteria of failure (e.g. when the demand exceeds the capacity) but do not model, as stated above, the essential converging process of events leading to the total failure/collapse of a system. For instance, in an excellent review paper by Valdez et al[2], the authors, among other important issues, discuss topological and overload models when the failure of the node with the highest connectivity or overload, respectively, is more likely to trigger a cascade.

On the contrary, and in addition to existing literature, in the current paper, we

suggest the innovative approach to modelling cascading failures from a different probabilistic viewpoint based on relevant self-exciting point processes that explain a possible mechanism of a cascade development.

For definiteness, where appropriate, we will mostly use the term 'defect' reserving "failure" for the whole system malfunction. The probability of a next event in a self-exciting process is increasing with the number of events previously experienced, which is, obviously, the case in

cascading failures modelling. However, can it result in a cascading pattern of events leading abruptly in the overall failure/collapse?

The answer to this question is "yes" when it is modelled by *bursting* point processes meaning that at some point of time (random) the process *explodes* with the infinite number of failures (almost surely). Obviously, in applications, for using our approach, the system should consist of a large number of components, which is the case, e.g., for large power grids on a national or regional level. In this sense and due to other assumptions, our approach might be oversimplified from a practical point of view. However, it gives probabilistic explanation of a bursting effect in cascading failures. It also sets the grounds for further developments and relevant illustrations. It is important to stress once more that cascading is usually triggered by some initial event after which the grid becomes vulnerable, and the cascading process can develop.

Two types of bursting point processes will be discussed: the geometric-type processes (Finkestein[11], Finkelstein and Cha[12]) with stochastically decreasing inter-arrival times and the modification of the generalised Polya process (Badia et al[13], Cha and Finkelstein[14]). The corresponding settings will be described and the conditions for bursting of the processes will be discussed. The remark on the additive type of bursting processes (Hawkes process (Hawkes[15])) will be also given.

With regards to possible applications, our approach is probably oversimplified for modelling the flow of events in, e.g., real-life power grids (as, for instance, not considering the specific network topology). However, we believe that even in this general form it can be useful for overall modelling of the converging process of cascading failures and understanding the probabilistic nature of this interesting phenomenon.

The paper is organized as follows. In Section 2 we consider geometric type bursting processes when each subsequent cycle (inter-arrival time) is shorter than the previous one in a specified way. This describes the damage that failures of components create for the rest of a system. Section 3 describes the extended generalized Polya process as the model for cascading failures under the specific condition. Section 4 considers an application with the real cascading failure data set and provides numerical illustrations and analysis, whereas Section 5 concludes the paper.

2. Geometric-type processes

The classic renewal process models recurrent events with the same (i.i.d.) inter-arrival times (Ross[16], Finkelstein[11]). Thus, it cannot be directly used for the description of the setting to be considered here for non-i.i.d. (decreasing) inter-arrival times. However, the geometric process (Lam[17 18]) can be already used for modelling the sequence of stochastically decreasing (Shaked and Shanthikumar[19]) inter-arrival times with the 'increasing in rate' accumulation of defects that eventually can result in a 'global' failure/collapse of a large system. This failure can occur via two major scenarios. Either a system is just reaching 'gracefully' the critical threshold for remaining resources without collapse of an entire system (as can still happen in an electrical power grids), or the process starts to burst (see later) at some point and actually results in a collapse of a system 'practically instantaneously'.

Geometric process was previously effectively employed in reliability for modelling, e.g., the imperfect repair, as after each imperfect repair, the time to the next failure is stochastically smaller than the previous one (Wang and Pham[20], Nguyen at al[21], Kahle[22], Pérez-Ocón and Torres-Castro[23] to name a few). However, here we will interpret it in a more general way as just a sequence of the stochastically decreasing lifetimes between the consecutive defects. Another possible interpretation is when the tolerable degradation threshold is decreasing with each defect. But first, we give the basic definition of the stochastic intensity that characterises a point process.

Definition 1. The stochastic intensity (intensity process) $\lambda_t, t \geq 0$ of an *orderly/regular* point process $\{N(t),\ t \geq 0\}$ is defined as:

$$\lambda_t = \lim_{\Delta t \to 0} \frac{E[N(t, t+\Delta t)|H_{t-}]}{\Delta t} = \lim_{\Delta t \to 0} \frac{P(N(t, t+\Delta t) = 1|H_{t-})}{\Delta t}, \quad (1)$$

where $H_{t-} = \{N(s): 0 \leq s < t\}$ is an internal filtration (history) of the point process in $[0, t)$, *i.e.*, the set of all point events in $[0, t)$ and $N(t, t+\Delta t)$ represents the number of events in $[t, t+\Delta t)$.

It is well known that $\lambda_t, t \geq 0$, for the NHPP reduces to its rate $\lambda(t)$, whereas for the ordinary renewal process with the underlying absolutely continuous Cdf $F(t)$ and its failure rate $\lambda(t)$, we have: $\lambda_t = \lambda(t - S_{N(t-)})$, where $S_{N(t-)}$ is the time of the last renewal before t and $0 = S_0 < S_1 < S_2 \ldots$ are the corresponding arrival times.

In the following, throughout this paper, we let $\{T_n\}, n = 1,2,\ldots$ be a collection of independent lifetimes with the Cdfs $F_n(t)$ that are called cycles and interpreted as the inter-arrival times for the corresponding generalized renewal process

$$N(t) = sup\{n: S_n \leq t\}, \quad t \geq 0;\ S_n = \sum_{i=1}^{n} T_i, \quad S_0 = 0. \quad (2)$$

2.1 Geometric process

Assume the specific form of the Cdfs $F_n(t)$, namely

$$F_n(t) = F(a^{n-1}t), n = 1,2,\ldots, \quad (3)$$

where $F(t)$ is a baseline distribution. Then the defined process is called the *geometric process* (Lam[17 18]). When $a > 1$,

$$F_n(t) \leq F_{n+1}(t),\ t > 0, a > 1 \quad (4)$$

and, therefore, the inter-arrival times are stochastically decreasing, and the process is, obviously, converging in expectation ($lim_{n\to\infty} E\,[S_n] < \infty$), if the mean that corresponds to $F(t)$ is finite.

The stochastic intensity for the geometric process can be written as

$$\lambda_t = a^{N(t-)}\lambda\left(a^{N(t-)}(t - S_{N(t-)})\right).$$

In renewal theory, the expectation of the number of events in $(0, t]$, i.e., $E[N(t)] = M(t)$ plays a pivotal role. The corresponding renewal-type integral equation exists for this function in the case of the geometric process as well (Lam[18], Finkelstein[11])

$$M(t) = F(t) + \int_0^t M\big(a(t-x)\big)\, f(x)dx, \tag{5}$$

where $f(x) = dF(x)/dx$.

For the renewal process ($a = 1$), this function is finite for any fixed *t*. However, although intuitively it is not evident at all, for geometric process with $a > 1$, as shown in Braun et al[24], this function is infinite for all $a > 1$ and $t > 0$ (see also Finkelstein[25]). Moreover, this process 'explodes' with probability 1 (almost surely) at some finite random time $T < \infty$, if the variance that corresponds to $F(t)$ is finite. By this we mean the following:

$$T = \inf\{u: N(t) = \infty \text{ with probability 1 for all } t \geq u\}. \tag{6}$$

This explosion/bursting time can be found explicitly for the case of the exponential (with failure rate λ) baseline distribution that, obviously, has the finite variance. This is important for general understanding and applying in real-life problems. It follows from Braun et al[24] and Anderson[26] (pages 20-22) that in this specific case

$$P(T \leq t) = 1 - \sum_{k=1}^{\infty} C_{a,k} e^{-a^k t}$$

$$C_{a,k} = \prod_{h=1}^{k-1} \frac{1}{1-a^h} \lim_{n\to\infty} \prod_{j=1}^{n-k} \frac{a^j}{1-a^j}$$

Note that, for the point process, the infiniteness of the mean number of events in [0,t) for any $t > 0$ does not mean automatically that it is bursting in accordance with (6), as the former just describes a random variable with the expectation equal to infinity. We will consider the corresponding convergence properties in more detail for a more general case discussed in the next subsection.

Remark 1. It is well known (see, e.g., Anderson[26]) that the Markov pure birth process with transition rates λ_i (from state *i* to state $i+1$, $i = 0,1,2, \ldots$) explodes if

$$\sum_{i=0}^{\infty} \frac{1}{\lambda_i} < \infty\,. \tag{7}$$

which is, obviously, the case for the geometric process with the baseline exponential distribution (parameter λ) and $a > 1$ as $\lambda_i = a^i\ \lambda$. Thus, we have the following straightforward proposition.

Proposition 1*. If the baseline distribution of a geometric process is the exponential distribution and* $a > 1$*, then this process is exploding/bursting.*

What can explosion mean applications-wise? Assume that we have a system that, in principle, can tolerate a large number of defects. However, if they occur shortly one after another, it does not have sufficient time to react and eventually collapses. This happens during blackouts of countries or regions electricity power grids when this time can be just minutes, which for modelling can be considered as practically instantaneous (see the examples in the Introduction).

Consider two geometric processes with the same baseline distribution and different scaling values $a_2 > a_1 > 1$. Then

$$F(a_1^n t) < F(a_2^n t), n = 1,2,...$$

meaning that each cycle of the second process is stochastically smaller than that of the first process (in the sense of the usual stochastic order). Therefore, the second process will burst stochastically earlier than the first one. Furthermore, as the finite convolutions of the stochastically smaller variables is also stochastically smaller, then obviously

$$M_2(t) > M_1(t) \text{ and } T_2 <_{st} T_1. \quad (8)$$

where subindex, $i = 1,2$, refers to the number of the process, respectively.

One can consider more general processes with different scale factors on each cycle. As long as the conditions $a_i > 1, i = 1,2, ...$ and $\lim_{i\to\infty} a_i = a > 1$ hold, the process is bursting, as follows from Remark 1. Furthermore, due to Proposition 1 and the reasoning applied to the comparison of two geometric processes described above, we have the following result on the bursting of geometric process with non-exponential distributions.

Proposition 2. *Let the failure rate function $\lambda(t)$ that corresponds to the baseline distribution of the geometric process satisfy $\inf_{\{t\geq 0\}} \lambda(t) > 0$ and $a > 1$. Then the process is exploding/bursting.*

Proof. If the failure rate $\lambda(t)$ of the baseline distribution (with Cdf $F(t)$) satisfies $\inf_{\{t\geq 0\}} \lambda(t) > 0$, then there exists a constant failure rate λ_0 of an exponential distribution which satisfies $\inf_{\{t\geq 0\}} \lambda(t) > \lambda_0$. Then,

$$F_0(a^n t) < F(a^n t), n = 1,2,...,$$

where $F_0(t) = 1 - \exp\{-\lambda_0 t\}$. If $a > 1$, due to Proposition 1, the geometric process with exponential distribution having failure rate λ_0 is bursting. Now, each cycle of the geometric process with the baseline failure rate $\lambda(t)$ is stochastically smaller than the geometric process with exponential distribution having failure rate λ_0. Therefore, the geometric process with such baseline failure rate $\lambda(t)$ is bursting.

■

2.2 Process with geometrically decreasing degradation threshold

Assume now that the observable (continuously monitored or only at failure) internal deterioration process in a system $\{W_t, t \geq 0\}, W_0 = 0$, has independent increments and is characterized by the monotonically increasing sample paths. Then the lifetime of a system with wear described by this process, L can be defined via the corresponding survival function

$$P(L > t) \equiv \bar{F}(t, w) = P(W_t \leq w) \quad (9)$$

when the failure is defined as reaching/crossing the level w.

Assume that with each defect, the failure threshold w decreases as $a^i w, i = 1,2, ..., 0 < a < 1$, which models the decrease of the remaining resources after each defect. Then, similar to (4),

the following usual stochastic ordering (Shaked and Shanthikumar[19]) for the durations of cycles in this quasi-geometric process holds

$$F(t,w) \equiv F_1(t) < F(t,aw) \equiv F_2(t) < F(t,a^2w) \equiv F_3(t), \dots, a < 1. \quad (10)$$

The renewal-type equation (with respect to the renewal function $M(t,w)$) also holds. Indeed, denote by $f(x,w)$ the density that corresponds to $F(t,w)$. Then, similar to (5),

$$M(t,w) = F(t,w) + \int_0^t M\big((t-x,aw)\big) f(x,w)dx,$$

However, its analysis is more complex than that of (5), as here we have, in fact, two variables in the function $M(t,w)$. However, under certain assumptions, the infiniteness of this function, which is of our interest, can be proved. Note that, as mentioned above, there is quite and number of studies of conventional geometric process considered in the previous subsection, whereas the current model, to the best of our knowledge was introduced and discussed only in Finkelstein and Cha[27]. On the other hand, it can be more relevant in applications, where degradation is modelled by increasing stochastic process. Indeed, it describes the decrease of capacity of a system (e.g., electricity grid) with each event in the process, whereas the form of the corresponding distribution functions is just a consequence of this pattern.

Let the cycles (inter-arrival times) $\{T_n\}, n = 1,2,\dots$ that are described by the Cdfs in (10) form the point process with geometrically decreased degradation threshold. Assume that the mean that corresponds to the baseline $F(t,w)$ is finite and denote it by μ_1. Then the subsequent means $\mu_i, i = 2,3, \dots$ are obviously also finite. Assume that our process is converging in the mean in the following sense:

$$\sum_{i=1}^{\infty} E[T_i] = \sum_{i=1}^{\infty} \mu_i = b < \infty \quad (11)$$

Note that, assumption (11) holds automatically for the geometric process (3) and for the case of Markov pure birth processes when (7) holds.

Example 1. Consider the homogeneous Poisson process of discrete deterioration with a sufficiently large intensity λ, so that the discrete threshold w in this case can be considered approximately as continuous. Let $1/\lambda = d$ be the corresponding mean of the inter-arrival times for the Poisson process. Then $\mu_i = a^{i-1}wd, i = 1,2\dots$ Thus, (11) holds and the process becomes approximately the geometric one.

Example 2. For a stationary gamma process of deterioration with parameters v and β, its expectation is linear $E[W_t] = vt/\beta$. Therefore, the expected time to reach the threshold is approximately $\beta w/v$. This approximation is becoming 'better' with increasing β (coefficient of variation is decreasing). Thus, similar reasoning as for the Poisson process of degradation holds.

Denote $\sum_{i=1}^{\infty} T_i \equiv S$ with the corresponding Cdf $G(t)$.

Theorem 1. *Assume that the governing lifetime Cdf* $F(t,w)$ *in (10) is absolutely continuous, strictly positive and strictly increasing for all* $t > 0$. *Let the point process* $N(t),\ t \geq 0$, *be converging in the sense of (11). Then*

$$E[N(t)] \equiv M(t,w) \text{ is infinite for all } t > 0.$$

As the proof of this result is in the spirit of that in Finkelstein and Cha[27], it is deferred to the Appendix. Note that this theorem does not yet describe burstiness and refers only to the infiniteness of $E[N(t)]$. However, as Equation (A2) holds for any n it also means that, similar to geometric process, this process is bursting at a random time T, which is finite with a positive probability (see definition (6)). For showing that this probability is 1, assume that the variance that corresponds to $S = \sum_{i=1}^{\infty} T_i$ denoted by σ_S^2 is finite, which should naturally follow from the assumption on finiteness of the variance that correspond to $F(t,w) \equiv F_1(t)$ and the model (10) (at least, for some processes of deterioration). The following simple but meaningful result holds.

Theorem 2. *Let the point process* $N(t),\ t \geq 0$, *be converging in the sense of (11) and* σ_S^2 *be finite. Then the process with geometrically decreasing degradation threshold described above is bursting at time T, which is finite with probability 1.*

Proof. Let us provide the lower bound for the probability $P(T < b + y), y > 0$. In a similar manner as in Braun et al[24] for 'ordinary' geometric process, using now Chebyshev's inequality for the case of a process with geometrically decreasing failure threshold considered here,

$$P(T < b + y) \geq 1 - \frac{\sigma_S^2}{y^2}, \tag{12}$$

which, due to monotone convergence theorem implies (for sufficiently large y) that

$$P(T < \infty) = 1\,. \tag{13}$$

Thus, this process under the given assumptions, similar to the geometric one, explodes at a finite random time T: $N(t) = \infty$ with probability 1 for all $t > T$.

■

It can be easily seen from Example 1 that the finiteness of the variance σ_S^2 holds in this case (Poisson process of deterioration), as the considered process is approximately geometric. For the stationary gamma process of deterioration, along with (11) the finiteness of σ_S^2 also holds.

Obviously, similar to our considerations at the end of the previous subsection devoted to the geometric processes, it holds that

$$F(t, a_1^n w) < F(t, a_2^n w),\ a_2 < a_1 < 1, n = 1,2,\ldots \tag{14}$$

meaning that each cycle of the second process is stochastically smaller than that of the first one. Then (8) holds for this case as well.

3. GPP-type point processes

Definition 2. (Cha[28], Cha and Finkelstein[14]). *A counting process* $\{N(t), t \geq 0\}$ *is called the Generalized Polya Process (GPP) with the set of parameters* $(\lambda(t), \alpha, \beta)$, $\alpha \geq 0$, $\beta > 0$, *if* $N(0) = 0$ and its stochastic intensity is given by

$$\lambda_t = (\alpha N(t-) + \beta)\lambda(t). \tag{15}$$

The GPP with $(\lambda(t), \alpha = 0, \beta = 1)$ reduces to the NHPP with the rate $\lambda(t)$. Thus, $\lambda(t)$ in this case can be considered as some baseline failure rate of a system before occurrence of the first event. Consider, for example, a system with a constant failure rate λ and a shock process effecting this item. i.e., with each shock its failure rate increases by $\alpha\lambda$. Then the stochastic intensity that characterises performance of this item in a random shock environment will be given by (15) with $\beta = 1$. Obviously, (15) defines the self-exciting point process as it is clearly seen that the probability of occurrence of the current event is increasing in the number of the previous events.

The probability of occurrence of n events for the GPP is given in Cha[28] as

$$P(N(t) = n) = \frac{\Gamma\left(\frac{\beta}{\alpha} + n\right)}{\Gamma\left(\frac{\beta}{\alpha}\right) n!}(1 - exp\{-\alpha\,\Lambda(t)\})^n (exp\{-\alpha\,\Lambda(t)\})^{\frac{\beta}{\alpha}}, n = 0,1,2,\ldots, \tag{16}$$

where $\Lambda(t) \equiv \int_0^t \lambda(u)du$ is the cumulative failure rate in reliability interpretation. It can be also easily seen from (16)

$$E[N(t)] = \sum_1^n nP(N(t) = n) = \frac{\beta}{\alpha}(exp\{\alpha\,\Lambda(t)\} - 1). \tag{17}$$

On the other hand, its expectation (17) is finite for any $t > 0$, thus, obviously, there is no bursting.

As we are interested in modelling bursting/collapsing point processes, a natural question arises: how Definition 2 should be modified to account for this possibility of bursting. Obviously, the dependence on history (which is a linear function of the number of events in the history in (15)) should be more 'intense' (e.g., a power law or exponential) in order to achieve this possibility.

Definition 3. *A counting process* $\{N(t), t \geq 0\}$ *is called the Extended Generalized Polya Process (EGPP) with* $(\lambda(t), r(t))$, *if* $N(0) = 0$ and its stochastic intensity is given by

$$\lambda_t = r(N(t-))\lambda(t), \tag{18}$$

where $r(t)$ is a monotone, absolutely continuous function in $[0, \infty)$ with $r(0) = 1$.

The latter condition is just for the useful interpretation for $\lambda(t)$ to be interpreted as an initial failure rate of a system at the start of the cascading process.

The EGPP was introduced and characterized in Badia et al[13]. However, here, having in mind the cascading failures modelling, we are mostly interested in its bursting properties that requires a more detailed discussion in this respect. When $r(t)$ is decreasing, then the 'rate' with which the history influences the future is negative, i.e., $r'(t) < 0$. For another example, let us relax the assumption of absolutely continuity and set

$$r(t) = \begin{cases} g(t), 0 \leq t < c \\ a, t \geq c, \end{cases}$$

where $g(t)$ is an arbitrary absolutely continuous, increasing function in $[0, c)$. Then the resulting stochastic process in $[c, \infty)$ will be the mixed Poisson process with the baseline rate $\lambda(t + c)$, and the mixing distribution that is defined by (16) for $t = c$ (for the specific case of the GPP in $[0, c)$). Thus, in these cases, obviously, there is no bursting.

On the other hand, when $r(t)$ is increasing in $[0, \infty)$, the 'rate' with which the history influences the future of the point process is positive, as $r'(t) > 0$. Note that the GPP with $r(t) = \alpha t + \beta$ and $r'(t) = \alpha$ is not bursting; then $r'(t)$ is likely to increase to acquire the bursting property, which is our goal. To see this and obtain conditions for burstiness consider first the case of a constant baseline $\lambda(t) \equiv \lambda$.

From our reasoning in the previous section (see equation (11)) and considering (18) for this specific case, the following series of the means of the corresponding *exponentially distributed* inter-arrival times $T_i, i = 1,2, \ldots$ (for the process EGPP$(\lambda, r(t))$ to burst) should converge

$$\sum_{i=1}^{\infty} E[T_i] = \sum_{i=0}^{\infty} \frac{1}{\lambda r(i)} = b < \infty, \quad b > 0\,, \tag{19}$$

where, for definiteness and reliability interpretation, let $r(0) = 1$, which corresponds to $\beta = 1$ in (15). Thus, we see that this specific case can be considered in the same manner as in the previous section not using some general results from probability theory. Furthermore, the convergence for the variance of the sum of exponentially distributed inter-arrival times discussed for the geometric-type processes follows now automatically in this specific case. Moreover, convergence $\sum_{i=1}^{\infty} E[T_i]$ as the condition for bursting follows trivially for the more general and relevant for applications case when $\lambda(t)$ is increasing showing the aging property of the underlying baseline distribution. Let us rewrite this condition without linking it to the specific exponential case (19)

$$\sum_{i=0}^{\infty} \frac{1}{r(i)} = d < \infty, d > 0. \tag{20}$$

As EGPP$(\lambda, r(t))$ is a homogeneous Markov pure birth process, it follows, e.g., from Gikhman and Skorokhod[29] (page 323) that this process is explosive if and only if condition (19) holds. Moreover, it is proved in Badia et al[13] (Proposition 2) that the same result holds for EGPP $(\lambda(t), r(t))$ being a direct consequence of the result for the EGPP $(\lambda, r(t))$. The corresponding 'construction' based on the EGPP$(\lambda, r(t))$ was discussed in detail in this paper. It was also shown that the time of explosion T is finite as it was for the geometric-type processes of the previous section.

The distribution of the time of explosion T can be analysed using the distributions of arrival times for the EGPP$(\lambda, r(t))$ obtained in Badia et al[13]. However, computationally it can be rather intensive and it is more reasonable for illustrations to use the direct simulation results.

What are the simplest illustrative candidates for the function $r(t)$ that satisfy condition (19). The first choices are, obviously,

$$r(n) = (1 + n)^{\delta}\,, \delta > 1, \tag{21}$$

$$r(n) = q^n, q > 1. \tag{22}$$

For both cases we have $r(0) = 1$ and thus, $\lambda(t)$ in (18) can be interpreted as an initial failure rate of a system at the start of the cascading process. We see that the larger values of n, q, δ for these models result, obviously, in a smaller bursting time (in the sense of the mean value).

Remark 2. As it was mentioned, condition (20) guarantees bursting for increasing and decreasing (asymptotically converging to a positive constant) $\lambda(t)$. The following reasoning explains intuitively how the classical condition for burstiness of the homogeneous Markov pure birth process, (19) is 'working' for EGPP $\big(\lambda(t), r(t)\big)$ in the case when the failure rate $\lambda(t)$ is decreasing to 0. Recall that $\lambda(t)$ is the baseline failure rate of the initial lifetime distribution and thus, should approach 0 'slowly' as

$$\int_0^\infty \lambda(u)du = \infty.$$

This means that, the finiteness of the corresponding sum (similar to (19)-(20)), is defined by $r(N(t-))\lambda(t)$ which is the increasing to ∞ (almost surely) when $t \to \infty$. If $r(n)$ is given, e.g., by (21) or (22), multiplying it by the function that is approaching 0 at ∞ slower than $1/t^{1+\varepsilon}$ (whatever small $\varepsilon > 0$ is) will not change the condition for burstiness (20). On the other hand, the strict proof of a more general result, as mentioned, can be found in Badia et al[13].

Remark 3. Let $\beta = 1$. Then equation (15) defines the *multiplicative* model of self-exciting point process:

$$\lambda_t = (\alpha N(t-) + 1)\lambda(t) = \lambda(t) + \big(\alpha N(t-)\big)\lambda(t), \tag{23}$$

where $\lambda(t)$ can be also interpreted as the initial failure rate of a system. On the other hand, the *additive* model (compare with (23)) can be also defined via its stochastic intensity as

$$\lambda_t = \lambda(t) + \alpha N(t-)\,, \tag{24}$$

which, in fact, is the special case of the Hawkes process (Hawkes[15]) for the excitation function being a constant. Let, first, as previously $\lambda(t) = \lambda$ and the process is again homogeneous pure birth process, which is non-explosive as

$$\sum_{i=1}^{\infty} E[T_i] = \frac{1}{\lambda}\sum_{0}^{\infty} \frac{1}{1+i\alpha} = \infty\,. \tag{25}$$

However, if the influence on the history is more pronounced, then it can burst similar to the EGPP defined by (18). Indeed, if we substitute $\alpha N(t-)$ by some monotone function of $N(t-)$ denoted by $s(t), s(0) = 0$, then similar to (11) and taking into account (16) and (19), the condition for bursting is

$$\sum_{i=1}^{\infty} E[T_i] = \frac{1}{\lambda}\sum_{0}^{\infty} \frac{1}{1+s(i)} < \infty\,. \tag{26}$$

As examples, due to (21) and (22): $s(n) = (1+n)^{\delta} - 1;\ s(n) = q^n - 1$.

Relation (26) can be written in a 'pure' and slightly modified as

$$\sum_{i=1}^{\infty} \frac{1}{s(i)} < \infty. \tag{27}$$

This condition, obviously, holds for a more general case when the baseline $\lambda(t)$ is increasing. To consider the case of arbitrary $\lambda(t)$, the approach developed in Badia et al[13] should be used.

The cascading sequence of events modelled by the bursting process starts with the triggering/initiating event. Thus, the subsequent modelling of a cascade is conditional on this event, which can be of external (hurricane, tsunami) or of internal (e.g., unexpected increase in demand in power or dramatic operational error). How can our approach be helpful in analysis of the possible collapse of a grid? We believe that the analysis of the possible significant failures could be made or corresponding simulations performed in order to identify possible sequences that can result in geometric-type (in a general sense) reductions in remaining resources.

Obviously, if we have two EGPPs with $r_1(t) \geq r_2(t)$, then, if the second process is bursting, then the first one will burst as well.

4. Numerical study and real data analysis

4.1 Numerical illustrations

In this initial subsection, general cascading failures patterns for the geometric process and the EGPP are illustrated. Further detailed real data analysis and simulations are presented in the next two subsections.

Geometric process

Consider the geometric process with $F_n(t) = F(a^{n-1}t), n = 1,2,\ldots,$ with $F(t) = 1 - \exp\{-t\}$. We compare two cases with $a = 2$ and $a = 5$. For these two cases, five sample trajectories of $N(t)$ have been generated respectively (see Figure 1).

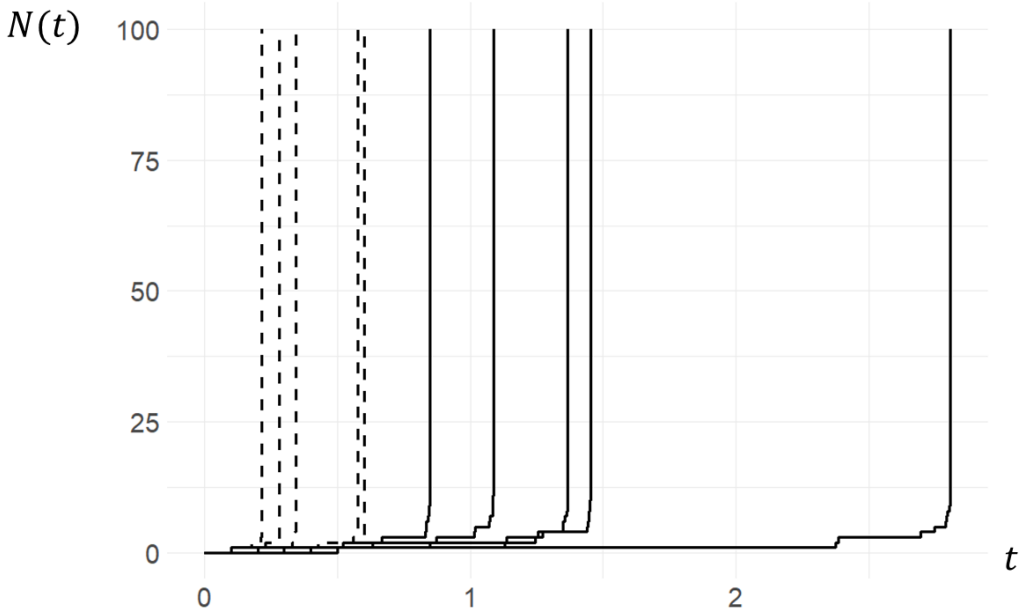

Figure 1. Five sample trajectories of $N(t)$ for $a = 2$ (solid lines) and $a = 5$ (dashed lines)

As can be seen from Figure 1, the times of explosion/bursting are finite and they illustrate stochastic ordering for these two cases defined by (8).

EGPP

Consider the EGPP with $\lambda_t = r(N(t-))\lambda(t)$, where $r(n) = (1+n)^{\delta}$ and $\lambda(t) = 1, \forall t > 0$. We compare two cases with $\delta = 2$ and $\delta = 4$. As for the geometric process, for these two cases, five sample trajectories of $N(t)$ have been generated respectively (see Figure 2).

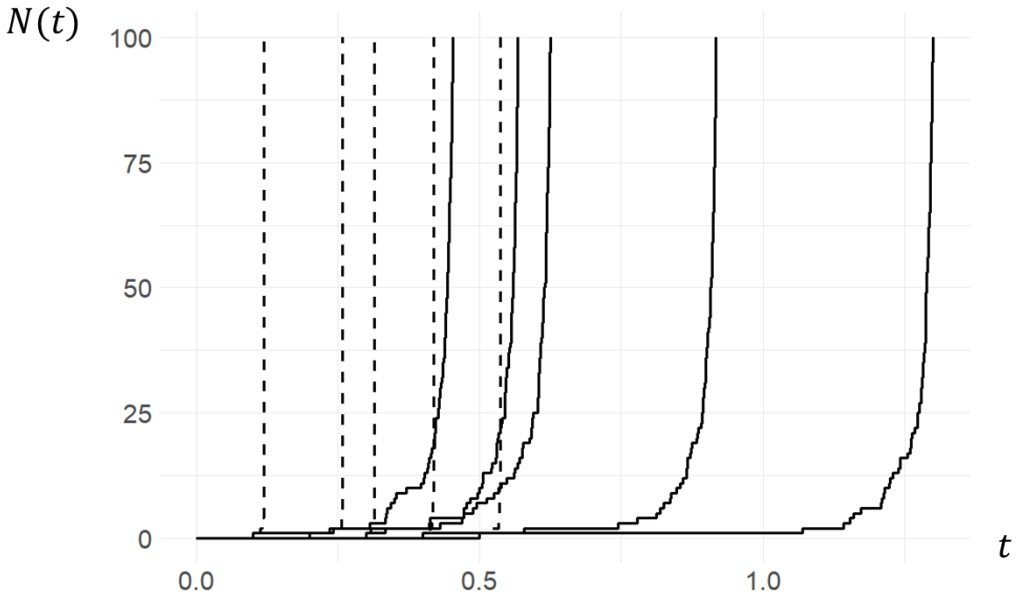

Figure 2. Five sample trajectories of $N(t)$ for $\delta = 2$ (solid lines) and $\delta = 4$ (dashed lines)

Similar to Figure 1, the times of explosion/bursting in Figure 2 are finite and they illustrate stochastic ordering for these two cases defined by (8).

4.2 Analysis of a real cascading failure data set

In this subsection, we apply the developed models to a real cascading failure data set from a public power-grid. The Western Systems Coordinating Council (WSCC) blackout of 10 August 1996 was a large-scale transmission disturbance that progressed from an initial localized fault to a rapidly developing cascade of line outages across parts of the western North American grid. Eakeley EC et al[30] in the NERC report record the event sequence and absolute timestamps; the official timeline shows a few early, isolated faults in the afternoon followed by an escalation phase beginning near 15:47 local time and a highly concentrated sequence of protective trips and line openings clustered around 15:48 ~ 15:49 during the cascade stage. The detailed event times reproduced from that report are presented in Table 1.

Event number	Time	Event number	Time
1	14:06:39.769	28	15:48:54.622
2	14:52:37.156	29	15:48:54.700
3	15:42:03.139	30	15:48:54.703

4	15:47:29.000	31	15:48:54.765
5	15:47:36.000	32	15:48:54.825
6	15:47:40.000	33	15:48:54.846
7	15:47:44.000	34	15:48:54.936
8	15:47:52.000	35	15:48:54.938
9	15:48:09.000	36	15:48:55.000
10	15:48:52.588	37	15:48:55.141
11	15:48:52.613	38	15:48:55.405
12	15:48:52.618	39	15:48:58.496
13	15:48:52.632	40	15:48:58.803
14	15:48:52.641	41	15:48:59.000
15	15:48:52.682	42	15:48:59.341
16	15:48:52.740	43	15:48:59.492
17	15:48:52.778	44	15:49:00.000
18	15:48:52.782	45	15:49:07.140
19	15:48:52.878	46	15:49:13.315
20	15:48:53.000	47	15:49:13.405
21	15:48:53.255	48	15:49:14.000
22	15:48:53.622	49	15:49:20.830
23	15:48:53.649	50	15:49:45.271
24	15:48:53.708	51	15:49:48.000
25	15:48:53.930	52	15:49:59.723
26	15:48:54.415	53	15:50:00.000
27	15:48:54.576	54	15:54:00.000

Table 1. Sequence of significant events during the August 1996 WSCC blackout.

Operationally, the disturbance evolved as an initial fault and subsequent protection actions that permitted an overload-and-trip cascade; many outages are reported within seconds of one from another once the cascading phase began. This tight clustering of outage timestamps — a rapid, exponential-like rise in cumulative line trips over a short time window — makes the 1996 event a canonical example for studying bursty cascade dynamics and for testing point processes-based stochastic models of explosion/bursting. For these reasons we use the NERC event-time chronology (Table 1) as the empirical event-time series for model fitting.

Often, the bursting process can start with the triggering/initiating event such as unexpected increase in demand in power or dramatic operational error/fault as in this and many other real data sets. However, the triggering/initiating event is mostly not clearly observed and, as can be seen from the data set in Table 1, the exact timestamp of this initiating event is not recorded. Due to this reason, the observation of sequential cascading failures often starts from the occurrence time of the first event.

The (time-truncated, starting from 5950 sec.) graph of the cumulative number of failures $N(t)$ for the original data in Table 1 is provided in Figure 3, where the time (in sec.) represents the elapsed time since the occurrence of the first event. Note that, in the graph of the original data set, the so-called 'cascade phase-out' stage is observed, because the rate of failures at this stage slows down as a significant number of components have already failed and, accordingly, possible failure transition paths are almost disconnected (Sami and Naeini[31]). This phenomenon is very typical and common in many cascading failure real data (see Dobson et al[32], Wang et al[33]). In the analysis of cascading failure data analysis, the first precursor and the second escalation stages are the main interest because most of the failures occur in these two stages and the 'explosion' occurs at the end of these two stages (see, e.g. Dobson et al[32]). In our analysis of the cascading failure data given in Table 1, as we are also interested in the time until the explosion, the last 16 failures belonging to the cascade phase-out stage are deleted from the data set and the cascading failures until the time of explosion (which contains the first 38 failures) has been analysed. This truncated data set is depicted in Figure 4.

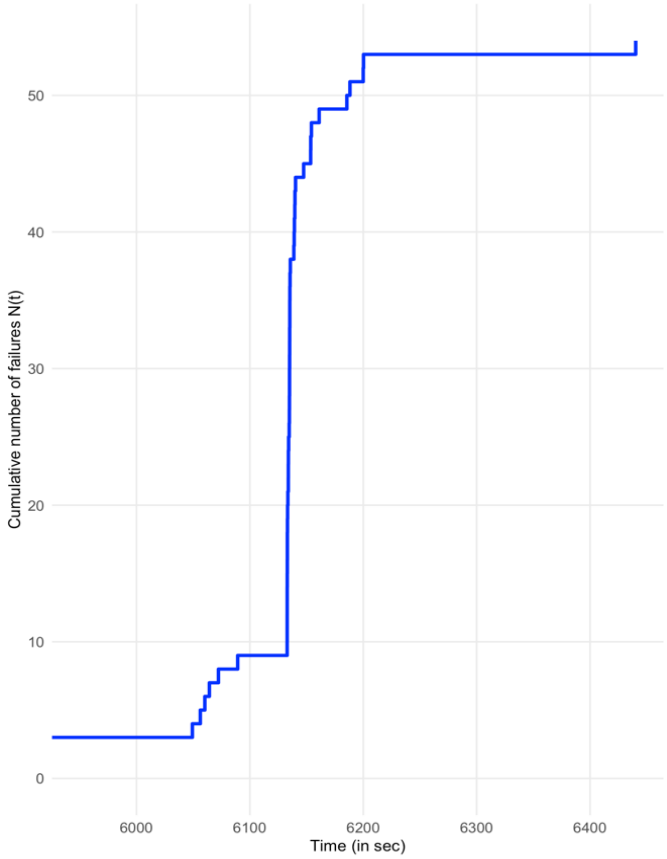

Figure 3. The graph of the cumulative number of failures in August 1996 WSCC blackout (original data)

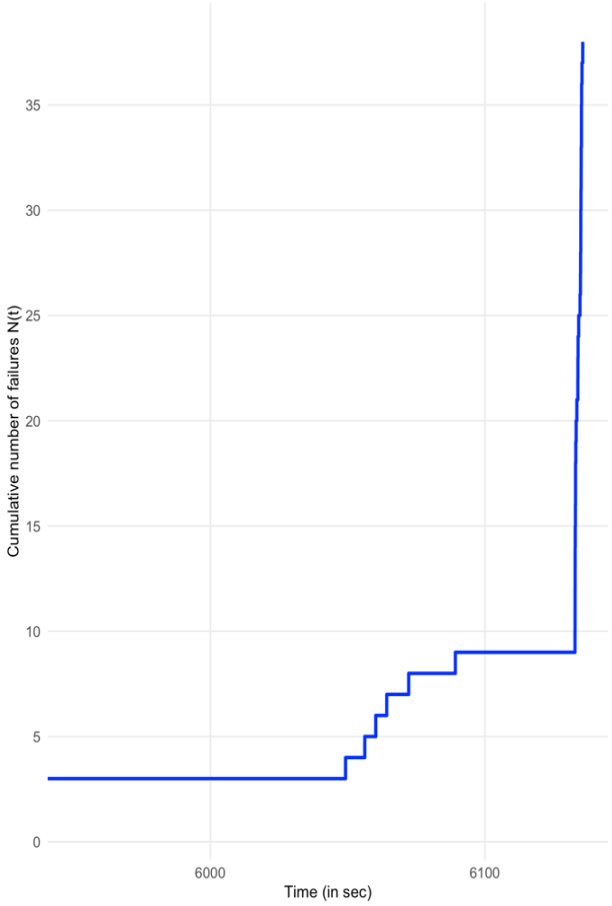

Figure 4. The graph of the cumulative number of failures in August 1996 WSCC blackout (truncated data)

To fit the data set, we consider

(i)The geometric process with $F_n(t) = F(a^{n-1}t), n = 1,2,\ldots,$ with $F(t) = 1 - \exp\{-\lambda t\}$.

(ii)The EGPP with $\lambda_t = r(N(t-))\lambda(t)$, where $r(n) = (1+n)^{\delta}, \delta > 1$

(iii)The EGPP with $\lambda_t = r(N(t-))\lambda(t)$, where $r(n) = q^n, q > 1$

In addition, observing relatively small number of failures in the first precursor stage and early escalation stage, a model with faster escalation effect could be more effective. Thus, in addition to the models (i)-(iii), we also consider the following EGPP model by increasing the power of n in the model in (ii):

(iv)The EGPP with $\lambda_t = r(N(t-))\lambda(t)$, where $r(n) = (1+n^3)^{\delta}, \delta > 1$

Note that, for each n, $r(n)$ in (iv) is larger than $r(n)$ in (ii) and, accordingly, the EGPP model in (iv) is also explosive.

As mentioned before, the sequential cascading failures can mostly be observed from the occurrence time of the first event, because the triggering/initiating event is not clearly observed, which also corresponds to the data set in Table 1. Therefore, when we apply the EGPP model, the baseline intensity $\lambda(t)$ should be specified as $\lambda(t) = \lambda, \forall t \geq 0$. Then, just after the occurrence of the first event, $N(t-) = 1$, the stochastic intensity in the models (ii)-(iv) can

be completely specified and the likelihood can be constructed without difficulty (even though one does not know the starting point of the process). For the truncated data set, the likelihood constructed for the EGPP models in (ii)-(iv) with $\lambda(t) = \lambda, \forall t \geq 0$, is given by

$$L = \prod_{i=2}^{38} exp\left\{-\int_{t_{i-1}}^{t_i} r(i-1)\lambda(u)du\right\} r(i-1)\lambda(t_i)$$

$$= \prod_{i=2}^{38} exp\{-[t_i - t_{i-1}]r(i-1)\lambda\} r(i-1)\lambda$$

as $N(t-) = i-1$, for $t_{i-1} < t \leq t_i$. For the geometric process, the likelihood is given by

$$L = \prod_{i=2}^{38} \left[a^{n-1} f\left(a^{n-1}(t_i - t_{i-1})\right)\right],$$

where $f(t) = F'(t) = \lambda \exp\{-\lambda t\}$ is used. For the estimation of the parameters, the MLEs maximizing the log-likelihood have been numerically obtained and the results of the estimation are summarized in Table 2.

Model	MLE	$\hat{l}$	AIC	BIC
Geometric	$\lambda = 0.0018, a = 1.308$	-82.7756	169.5511	172.7730
EGPP with $r(n) = (1+n)^{\delta}$	$\lambda = 0.00002, \delta = 3.854$	-40.9969	85.9937	89.2156
EGPP with $r(n) = q^n$	$\lambda = 0.0018, q = 1.308$	-82.7756	169.5511	172.7730
EGPP with $r(n) = (1+n^3)^{\delta}$	$\lambda = 0.00009, \delta = 1.149$	-39.4335	82.8669	86.0888

Table 2. Estimation results for the August 1996 data

Observe that the stochastic intensity for the geometric process in (i) is given by

$$\lambda_t = a^{N(t-)}\lambda, t > 0,$$

which is the same as that in the EGPP model in (iii). This is why the estimated parameters for these two models in Table 2 are the same. Based on the AIC and BIC, the EGPP with $\lambda_t = r(N(t-))\lambda(t)$, where $r(n) = (1+n^3)^{\delta}$, $\delta > 1$, outperforms the other models.

In Figure 5, the graphs of the average of 100 simulated sample paths of the fitted models are provided. For each fitted model given in Table 2, 100 simulated sample paths have been generated and their average has been obtained to obtain the graphs in Figure 5. As can be seen from Figure 5, the best fitted model, the EGPP with $\lambda_t = r(N(t-))\lambda(t)$, where $r(n) = (1+n^3)^{\delta}$, $\delta > 1$, can effectively capture the observed escalation pattern of the real data.

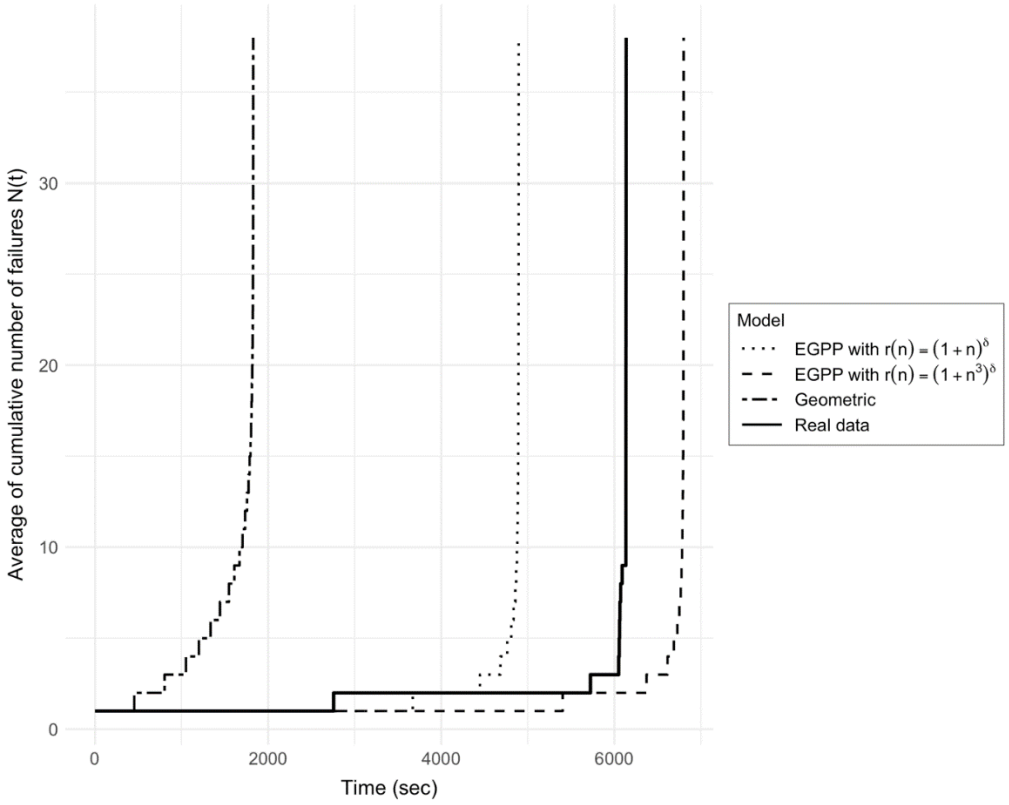

Figure 5. The average of 100 simulated paths of the fitted models

4.3 Monte-Carlo simulations

In this subsection, through Monte-Carlo simulations, the effect of model parameters on the distribution of explosion time will be studied and some comparison with Hawkes process will be performed.

In the following, the effect of model parameters is investigated for (i) geometric process with $\lambda(t) = \lambda, \forall\, t > 0$, and (ii) EGPP with $r(n) = (1+n)^{\delta}$ and $\lambda(t) = \lambda, \forall\, t > 0$,. In Table 3 (geometric process), to see the effect of model parameters λ, a on the distribution of explosion time, the mean, quartiles (Q1,Q2,Q3) and the interval $[p_{0.025}, p_{0.975}]$ (where p_{α} represents the value at which $(\alpha * 100)\%$ percentage of the observations lie below the value), which contains 95% of the observations from the corresponding distribution, are obtained.

a	λ	Mean	$Q1$	$Q2$	$Q3$	$[p_{0.025}, p_{0.975}]$
2	0.0001	10630.401	6178.947	9349.586	13655.193	(2807.258, 24836.995)
	0.0010	1012.526	586.333	891.451	1307.326	(274.456, 2453.925)
	0.0100	100.974	58.592	88.593	130.447	(26.436, 240.904)
3	0.0001	4862.498	2456.569	4090.642	6047.452	(858.843, 13363.438)
	0.0010	485.134	250.298	406.351	632.703	(97.993, 1348.464)
	0.0100	51.643	26.558	41.508	67.998	(7.867, 143.541)
5	0.0001	2497.163	1045.186	1963.195	3190.346	(302.734, 7817.346)
	0.0010	246.842	106.794	185.157	328.740	(30.922, 763.980)

	0.0100	24.689	10.101	19.259	33.451	(2.838, 77.120)
	0.0001	1400.161	562.821	993.839	1933.335	(144.985, 4606.201)
8	0.0010	144.681	53.325	105.376	191.223	(12.916, 475.858)
	0.0100	14.728	5.811	11.338	19.399	(1.728, 49.765)

Table 3. Summary statistics of T (explosion time) from 1000 Monte Carlo simulations - Geometric process

As can be seen from Table 3, as λ and a increase, the explosion time T becomes stochastically smaller. The changes of the distribution of explosion time T is more sensitive to the change of parameter λ.

In Table 4, for the EGPP, the effect of model parameters λ, δ on the distribution of explosion time has been investigated.

δ	λ	Mean	$Q1$	$Q2$	$Q3$	$[p_{0.025}, p_{0.975}]$
	0.0001	6662.370	4563.647	5984.384	8140.178	(2665.283, 13901.489)
2	0.0010	640.759	432.667	576.405	785.222	(258.866, 1343.538)
	0.0100	63.947	43.645	57.943	79.140	(26.604, 133.997)
	0.0001	1970.696	1075.205	1689.278	2443.398	(471.651, 5140.733)
3	0.0010	196.325	109.500	165.549	253.026	(53.815, 516.109)
	0.0100	20.788	11.234	16.881	26.786	(4.655, 55.378)
	0.0001	368.398	147.701	284.386	475.246	(41.925, 1208.088)
5	0.0010	36.442	14.520	26.898	48.620	(4.536, 116.348)
	0.0100	3.646	1.403	2.762	5.020	(0.411, 11.521)
	0.0001	40.086	13.670	27.069	55.600	(2.382, 140.716)
8	0.0010	4.132	1.264	2.825	5.697	(0.258, 14.75)
	0.0100	0.422	0.144	0.318	0.556	(0.027, 1.52)

Table 4. Summary statistics of T (explosion time) from 1000 Monte Carlo simulations – EGPP with $r(n) = (1+n)^{\delta}$

As can be seen from Table 4, as λ and δ increase, the explosion time T becomes stochastically smaller. Also in this case, the changes of the distribution of explosion time T is more sensitive to the change of parameter λ.

The stochastic models developed in this paper will be now compared with the well-known self-exciting process, the Hawkes process (Hawkes[34]). As there should be an explosion, we consider the following type of stochastic intensity that describes the Hawkes process, i.e.,

$$\lambda_t = \lambda(t) + \sum_{t_i:t_i<t} \phi(t-t_i), \text{ where } \phi(t) = a \cdot \exp\{bt\}. \quad (28)$$

For a comparative analysis, the Hawkes process model (28) is fitted to the truncated version of the cascading failure data given in Table 1 which involves the first 38 observations. Then, the fitted Hawkes process will be compared with the fitted models in Table 2. Thus, due to the same reason stated before, $\lambda(t)$ in (28) should be a constant function: $\lambda(t) = \lambda, \forall\, t > 0$. Then, the MLE's for λ, a, b in (28) are given by $\lambda = 0.0008, a = 0.564, b = -0.470$. For each

model, 1000 Monte Carlo simulations have been performed and distributions for the explosion time T have been obtained. The summary statistics for the explosion time T are given in Table 5.

Model	Mean	Q_1	Q_2	Q_3
Geometric	1912.69	1413.28	1786.54	2306.71
EGPP with $r(n) = (1+n)^{\delta}$	5067.35	2308.43	3988.65	6700.40
EGPP with $r(n) = (1+n^3)^{\delta}$	7030.41	3001.76	5368.62	9359.34
Hawkes with $\phi(t) = ae^{bt}$	782.84	16.07	23.03	699.64

Table 5. The summary statistics for the explosion time T

Considering the fact that the explosion time observed from the data is given by 6135, the Hawkes process tends to rather seriously underestimate it, as compared with the EGPP models. The graphs for the pdf's of the explosion time T are given in Figure 6.

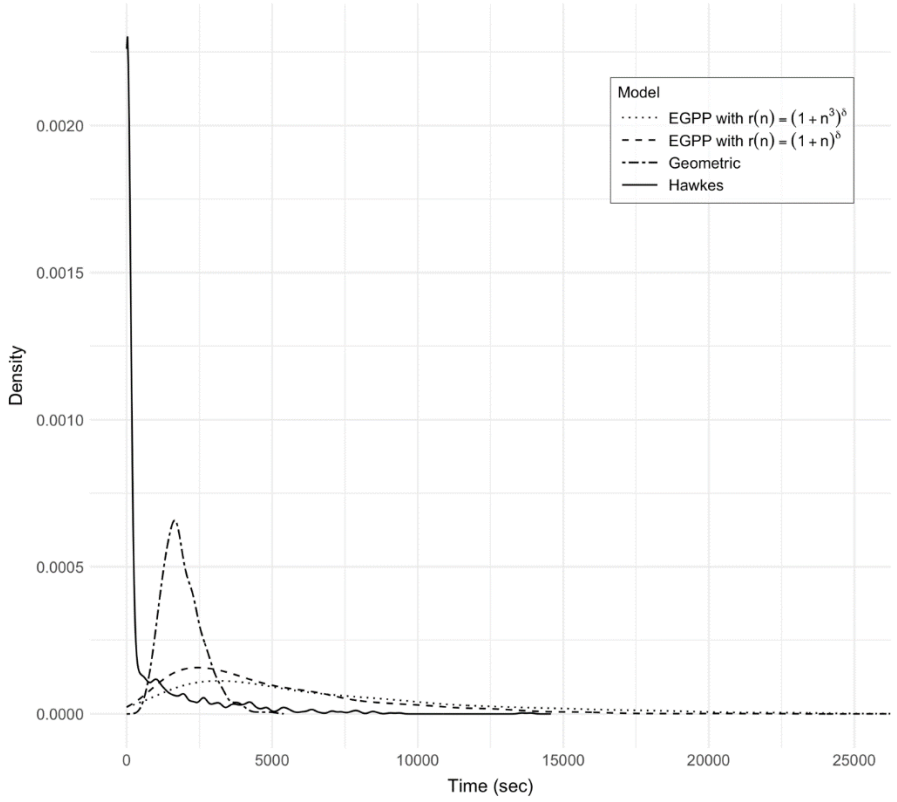

Figure 6. The graphs of the pdf's of the explosion time T

Finally, in Table 6, assuming that each model is the true model, the corresponding left and right tail risk probabilities have been obtained. As can be seen from Table 6, the right-tail risk probability for the Hawkes process model is relatively larger than those of the other models.

Model	$P(T > \mu + 3\sigma)$	$P(T > \mu + 2\sigma)$	$P(T > \mu + \sigma)$	$P(T < \mu - \sigma)$	$P(T < \mu - 2\sigma)$	$P(T < \mu - 3\sigma)$
Geometric	0.010	0.041	0.153	0.137	0.001	0.000
EGPP with $r(n) = (1+n)^{\delta}$	0.013	0.046	0.141	0.069	0.000	0.000
EGPP with $r(n) = (1+n^3)^{\delta}$	0.012	0.047	0.143	0.057	0.000	0.000
Hawkes with $\phi(t) = ae^{bt}$	0.026	0.059	0.119	0.000	0.000	0.000

Table 6. Tail risk summary

5. Concluding remarks

In this paper, distinct from the existing approaches in the literature, we discuss the innovative approach to modelling cascading failures from a different probabilistic viewpoint based on relevant self-exciting point processes that explain a *possible mechanism* of the cascade development.

This approach is probably oversimplified for modelling the flow of events in, e.g., real-life power grids (as, e.g., not considering the specific network topology). However, even in this general form it can be useful for overall modelling of the converging process of cascading failures and understanding the probabilistic nature of this interesting phenomenon.

As was stated in Remark 2: developed approach can be also helpful for identifying possible sequences of defects/failures in a system that can result in geometric-type (in a general sense) reductions in remaining resources. This can be done in the future applied research on some model grids at first. The goal of this study, however, is to justify the possibility of this further analysis.

The provided numerical illustrations and the detailed analysis of the real data set show that the proposed models can be effectively used for describing the real-life cascading sequences. The data set describing the Western Systems Coordinating Council (WSCC) blackout of 10 August 1996 was used for our analyses. This was a large-scale transmission disturbance that progressed from an initial localized fault to a rapidly developing cascade of line outages across parts of the western North American grid.

The comparison with the well-known self-exciting Hawkes process for the considered data set was also performed showing better description of the explosion time distribution. The possible explanation is in the fact that our models are multiplicative, whereas the Hawks process is additive. The latter is probably 'less suitable' for modeling the bursting phenomena. However, this topic needs further investigation.

Acknowledgements

The authors would like to greatly thank the reviewers for the helpful comments and constructive suggestions. The work of the third author was supported by the National

Research Foundation of Korea (NRF) grant funded by the Korea government (MSIP) (No. 2023R1A2C1003238).

Appendix

Proof of Theorem 1

It follows from (11) that there exists $\varepsilon > 0$ such that

$$G(b) \equiv P\left(\sum_{i=1}^{\infty} T_i \le b\right) = P(S \le b) > \varepsilon. \qquad (A1)$$

As

$$P\left(\sum_{i=1}^{n} T_i \le b\right) \ge P\left(\sum_{i=1}^{\infty} T_i \le b\right)$$

and

$$N(b) \ge n \Leftrightarrow \sum_{i=1}^{n} T_i \le b,$$

we have

$$P(N(b) \ge n) > \varepsilon, \ \forall n \ge 1. \qquad (A2)$$

It follows from (A1) that

$$M(b,w) = E[N(b)] = \sum_{i=1}^{\infty} P(N(b) \ge i) = \infty$$

Thus, $M(t,w)$ is infinite for $t = b$. However, as this function is not decreasing, *it is infinite for all* $t > b$. Furthermore,

$$S = \sum_{i=1}^{\infty} T_i = T_1 + \sum_{i=2}^{\infty} T_i \equiv T_1 + S_2$$

$$G(t) = \int_0^t f(x,w) G_2(t-x) dx,$$

where $G_2(t)$ is the Cdf of S_2.

Note that, as $f(x,w) > 0 \, for \, x > 0$ (assumption of Theorem 1) and $\sum_{i=2}^{\infty} E[T_i] = b - \mu_1$, similar to (A1), there exists $\delta_2 > 0$ such that

$$G_2(b-\mu_1) \equiv Pr\left(\sum_{i=2}^{\infty} T_i \le b - \mu_1\right) > \delta_2$$

Thus, there is some $\varepsilon_2 > 0$ such that

$$G(b-\mu_1) = \int_0^{b-\mu_1} f(x,w) G_2\,(b-\mu_1-x) dx > \varepsilon_2,$$

where μ_1 is the mean duration of the first cycle. Therefore, the expectations of the number of renewals in the interval of length $b - \mu_1$ is infinite. In the same manner, we can perform any number of the described above steps. Thus, after the n-th reduction of the interval, we arrive at $b - \sum_{i=1}^{n} \mu_i$, which by increasing n can be made as close to 0 as we wish. Furthermore, for the interval between any two consecutive points, $M(t, w)$ is non-deceasing in t, and, eventually, $M(t, w) = \infty$, *for all* $t \leq b$.

References

1. Pahwa S, Scoglio C, Scala A. Abruptness of cascade failures in power grids. *Scientific Reports* 2014; 4(1): 3694.

2. Valdez LD, Shekhtman L, La Rocca CL, Zhang X, Buldyrev SV, Trunfio PA, Braunstein LA, Halvin S. Cascading failures in complex networks. *Journal of Complex Networks* 2020; 8(2): cnaa013.

3. Swift AW. Stochastic models of cascading failures. *Journal of Applied Probability* 2008; 45(4): 907–921.

4. Lee H, Cha JH. Point process approach to modeling and analysis of general cascading failures models. *Journal of Applied Probability* 2016; 53(1): 174–186.

5. Schäfer B, Witthaut D, Timme M, Latora V. Dynamically induced cascading failures in power grids. *Nature Communications* 2018; 9(1): 1975.

6. Motter AE, Lai YC. Cascade-based attacks on complex networks. *Physical Review E* 2002; 66(6): 065102.

7. Liu D, Tse CK, Yang J, Zhang X. Revealing cascading failure vulnerability in evolving power grids with increasing penetration of inverter-based resources. *IEEE Transactions on Circuits and Systems I: Regular Papers* 2024; (99): 1–13.

8. Song B, Zhang ZH, Song YR, Jiang GP, Li YW, Su XP. Preferential redistribution in cascading failure by considering local real-time information. *Physics A: Statistical Mechanics and its Applications* 2019; 532: 121729.

9. Song X, Jia X, Dong Q, Xu D. System reliability under cascading failure models with different load effect modes. *Quality and Reliability Engineering International* 2023; 39(6): 2094–2112.

10. Zhao Y, Sun T, Liu Y. Reliability analysis of a loading dependent system with cascading failures considering overloads. *Quality and Reliability Engineering International* 2024; 40(3): 1182–1196.

11. Finkelstein M. *Failure Rate Modelling for Reliability and Risk*. London: Springer; 2008.

12. Finkelstein M, Cha JH. *Stochastic modelling for reliability (shocks, burn-in and heterogeneous populations)*. London: Springer; 2013.

13. Badia FG, Mercier S, Sanguesa C. Extensions of the generalised Polya process. *Methodology and Computing in Applied Probability* 2019; 21: 1057–1085.

14. Cha JH, Finkelstein M. *Point Processes for Reliability Analysis: Shocks and Repairable Systems*. London: Springer; 2018.

15. Hawkes AG. Hawkes processes and their applications to finance: a review. *Quantitative Finance* 2018; 18(2): 193–198.

16. Ross S. *Stochastic Processes*. New York: John Wiley; 1996.

17. Lam Y. Geometric process and the replacement problem. *Acta Mathematicae Applicatae Sinica* 1988; 4: 366-377.

18. Lam Y. *The Geometric Process and Applications*. World Scientific; 2007.

19. Shaked M, Shanthikumar J. *Stochastic Orders*. New York: Springer; 2007.

20. Wang H, Pham H. *Reliability and Optimal Maintenance*. London: Springer; 2006.

21. Nguyen DT, Dijoux Y, Fouladirad M. Analytical properties of an imperfect repair model and application in preventive maintenance scheduling. *European Journal of Operational Research* 2017; 256(2): 439–453.

22. Kahle W. Imperfect repair in degradation processes: a Kijima-type approach. *Applied Stochastic Modelling in Business and Industry* 2019; 35(2): 211–220.

23. Pérez-Ocón R, Torres-Castro I. A reliability semi-Markov model involving geometric processes. *Applied Stochastic Models in Business and Industry* 2002; 18(2): 157–170.

24. Braun WJ, Li W, Zhao YQ. Some theoretical properties of geometric and alpha-series processes. *Communications in Statistics, Theory and Methods* 2008; 37(9): 1483–1496.

25. Finkelstein M. A note on converging geometric-type processes. *Journal of Applied Probability* 2010; 47(2): 601–607.

26. Anderson WJ. *Continuous-Time Markov Chains*. New York: Springer; 1991.

27. Finkelstein M, Cha JH. On degradation-based imperfect repair and induced generalized renewal processes. *Test* 2021; 30(4): 1026–1045.

28. Cha JH. Characterization of the generalized Polya process and its applications. *Advances in Applied Probability* 2014; 46(4): 1148–1171.

29. Gikhman II, Skorokhod AV. *Introduction to the theory of random processes (translated from Russian by Scripta Technica, Inc.)*. Philadelphia: Ont; 1969.

30. Eakeley EC et al. *1996 System Disturbances. Review of Selected 1996 Electric System Disturbances in North America* NERC report; 2002.

31. Sami NM, Naeini M. Machine learning applications in cascading failure analysis in power systems: A review. *Electric Power Systems Research* 2024; 232: 110415.

32. Dobson I, Carreras BA, Newman DE. Branching process models for the exponentially increasing portions of cascading failure blackouts. In *Proceedings of the 38th annual Hawaii international conference on system sciences* 2005.

33. Wang et al. Wang Z, Scaglione A, Thomas RJ. A Markov-transition model for cascading failures in power grids. In *45th Hawaii international conference on system sciences (pp. 2115-2124) IEEE* 2012.

34. Hawkes AG. Spectra of some self-exciting and mutually exciting point processes. *Biometrika* 1971; *58*(1): 83-90.